Journal of Alloys and Compounds 510 (2012) 114–118

Contents lists available at SciVerse ScienceDirect

Journal of Alloys and Compounds

journal homepage: www.elsevier.com/locate/jallcom

Electrochemical hydrogen absorbing properties of graphite/AB_5 alloy composite electrode

Xiaofeng Li*, Lizhen Wang, Huichao Dong, Yanghua Song, Haidong Shang

Henan Provincial Key Laboratory of Surface & Interface, Zhengzhou University of Light Industry, Zhengzhou, China 450002

ARTICLE INFO

Article history:
Received 8 August 2011
Received in revised form 2 September 2011
Accepted 5 September 2011
Available online 10 September 2011

Keywords:
Graphite
AB_5 alloy
Composite electrode
Electrochemical hydrogen absorbing property

ABSTRACT

Graphite is an inexpensive carbon material, but its hydrogen absorbing performance has attracted little attention. In this paper, in order to lower the cost of nickel metal-hydride (Ni-MH) battery, graphite is used as a hydrogen absorbing material in its negative electrode. The results of charge–discharge tests show that the graphite electrode has poor electrochemical hydrogen absorbing performance. The capacity of the graphite/AB_5 alloy (90 wt%) composite electrode is close to AB_5 alloy (298 mAh/g), but it has higher charge–discharge polarization and difficulty in activation. When graphite is modified with metal nickel powder by a simple ball milling process, the capacity of the composite electrode reaches to 315 mAh/g and its activation is accelerated. The results of electrochemical impedance spectroscopy (EIS) tests show that hydrogen diffusion in the modified composite electrode is more rapid than in AB_5 alloy, thereby resulting in lower charge–discharge polarization and better discharge performance at large currents.

1. Introduction

Hydrogen absorbing materials, including hydrogen absorbing alloy, carbon materials and chemical hydrides, have attracted great interests since hydrogen is believed to be an ideal pollution-free and renewable energy service in the future. Among these hydrogen absorbing materials, hydrogen absorbing alloy is mature in technology and has been widely used in nickel metal-hydride (Ni-MH) battery. But compared to the other hydrogen absorbing materials, it has some shortcomings such as high price, poor cyclic adsorption performance and slow hydrogen absorption/desorption kinetics.

Carbon materials such as supper-activated carbon, carbon nanotube and graphite nanofiber, has recently been used as hydrogen absorbing materials [1–10]. Different to the formation of metal hydride in hydrogen absorbing alloy, hydrogen absorption in carbon materials is based on weak van der Waals force between H_2 and the surface of the materials [3]. H_2 molecules lie in adsorbent interspaces with no interaction with the storage medium. In spite of the high stability in cycling operation and fast hydrogen sorption kinetics for hydrogen storage, these physisorption based storage processes have a low hydrogen capacity, due to insufficient binding between H_2 molecules and the adsorbent surface [4,5]. The hydrogen storage capacity of various carbon materials, including activated carbon, single-walled carbon nanohorn, single-walled carbon nanotubes and graphitic carbon nanofibers, was investigated by Xu et al. [6]. They reported that the hydrogen storage capacity of carbon materials was less than 1 wt% at 303 K and by lowering adsorption temperature to 77 K, the hydrogen storage capacity increased significantly to 5.7 wt% at a pressure of 3 MPa.

It was reported that some metal particles could assist the dissociation of hydrogen molecules to hydrogen atoms, thereby allowing atomic hydrogen to adsorb chemically at the defective sites of carbon materials [7,8]. Dǐaz and his coworkers [9] reported that the adsorption capacity of Pd-modified carbon nanofibres (CNF) increases close to 100% compared to the parent CNF (12.6 cm^3/g vs. 6.7 cm^3/g) at 0.1 MPa and 298 K. The hydrogen storage behaviors of platinum-supported multi-walled carbon nanotubes (MWNTs) were studied by Park et al. [10]. They reported that the hydrogen storage capacity of Pt/MWNTs reached 3.72 wt% at 298 K and 100 bar when the content of Pt was 5 wt%.

One important application of hydrogen absorbing materials is to be used as a negative electrode material in alkaline secondary batteries. $MmNi_{5-x-y-z}Co_xAl_yMn_z$ (AB_5, where Mm is misch metal) alloy is currently used in Ni-MH batteries. It has a specific capacity about 300–320 mAh/g and is quite expensive as it contains cobalt metal. Ni-MH batteries are widely used in today's power tools and portable applications, and in order to expand further their application fields such as a replacement for nickel–cadmium (Ni–Cd) batteries, a cost reduction of the batteries is necessary, since Ni–Cd batteries are more cheaper but have cadmium pollution.

Graphite is an inexpensive carbon material since it is wildly distributed in nature, but its hydrogen absorbing performance has attracted little attention because of its low specific surface area. In

* Corresponding author. Tel.: +86 371 63556510; fax: +86 371 63556510.
E-mail address: lixiaofeng@zzuli.edu.cn (X. Li).

0925-8388/$ – see front matter © 2011 Elsevier B.V. All rights reserved.
doi:10.1016/j.jallcom.2011.09.001

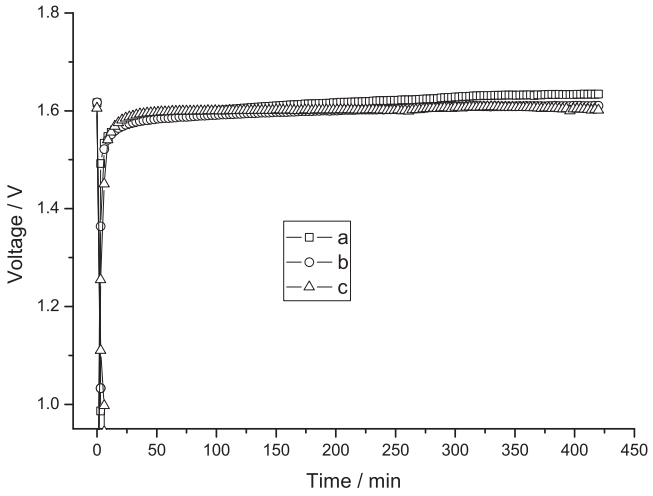

Fig. 1. Typical charge–discharge curves of the simulated batteries at a 0.2 C rate with the graphite electrodes (a) before ball milling (b) after ball milling for 2 h and (c) after ball milling for 5 h.

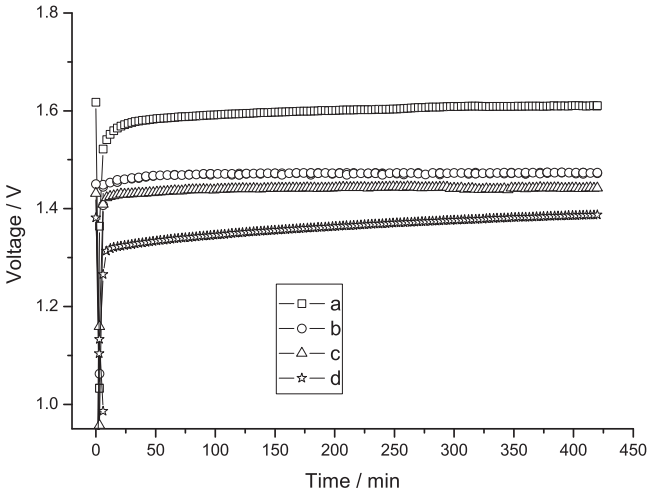

Fig. 2. Typical charge–discharge curves of the simulated batteries at a 0.2 C rate with the graphite electrodes (a) before modification (b) after ball milling with 10 wt% nickel powder for 2 h (c) after ball milling with 20 wt% nickel powder for 2 h and (d) after ball milling with 30 wt% nickel powder for 2 h.

this paper, in order to lower the cost of Ni-MH batteries, commercial graphite used as a conductive agent in manganese–zinc battery was chosen as a candidate for hydrogen absorbing material. It was modified with metal nickel powder by a simple ball milling process, and then it was mixed with AB_5 alloy to form the graphite/AB_5 alloy composite. The composite was used as a negative electrode material for the nickel base alkaline secondary batteries. Its electrochemical hydrogen absorbing properties were discussed in detail.

2. Experimental

Ball milling was performed by using a planetary ball mill with a 50-ml capacity stainless steel pot and 50 g stainless steel balls. A mixture of commercial graphite and metal nickel powder (nickel carbonyl, purity 99.5 wt%, particle size 1.5–3 μm) was added into the pot. The weight of the mixture was 2 g and 2 ml ethanol was also added into the spot as the grinding aid. The revolution speed was 300 rpm and the milling time was 2 h. The obtained powder was washed repeatedly with distilled water, and then dried at 65 °C for use. The surface morphology of nickel modified graphite was tested by using scanning electron microscopy (SEM).

The negative composite electrodes were prepared by filling a nickel foam substrate with a mixture of graphite (untreated or nickel modified), commercial $MmNi_{3.55}Co_{0.75}Al_{0.2}Mn_{0.5}$ alloy and polytetrafluoroethylene (PTFE) binder. The percentage composition of PTFE binder in the mixture is 8 wt%. The pasted electrodes were then dried at 65 °C and pressed to a thickness of 0.30 mm.

The electrochemical properties of the composite electrodes were investigated by using a 'sandwich-like' simulation battery in a 7 mol l^{-1} KOH solution at 25 °C. Two sintered $Ni(OH)_2$ electrodes obtained from a commercial supplier were placed on both sides and the composite electrode was positioned at the center. A cycling test was performed on the batteries by charging at a 0.2 C rate for 7 h and discharging at the same rate to a cut-off voltage 1.0 V for stabilizing their capacity. The electrodes were then charged at a 0.5 C rate for 2.6 h and discharged separately at a 1 C or 3 C rate to a cut-off voltage 0.8 V for high-power performance tests. Electrochemical impedance spectroscopy (EIS) tests were performed on the electrodes by using a Solartron Electrochemical Interface model SI1287.

3. Results and discussion

Firstly, commercial graphite was ball milled for 2 h or 5 h. The graphite electrodes were prepared with the same method as the composite electrodes and their electrochemical properties were investigated. Fig. 1 shows the charge–discharge curves of the simulated batteries with the graphite electrodes. It is clear that the graphite electrodes have poor electrochemical hydrogen absorbing performance, since all the discharge curves drop vertically and the discharge process finishes in several minutes. As shown in Fig. 2, when graphite was modified with metal nickel powder, the charge voltage of the simulated batteries declines with the increase in the addition amount of nickel powder, but the discharge process lasts still less than 10 min. These results seem to indicate that the electrochemical reduction of H_2O molecule to H atom on the surface of the graphite electrodes is improved by metal nickel, but there is still insufficient binding between H_2 molecules (or H atoms) and the graphite surface, thereby resulting in a poor discharge capacity.

Next, the composite electrode of graphite/AB_5 alloy (90 wt%) was prepared and its electrochemical properties were tested. As shown in Fig. 3, its discharge capacity (296 mAh/g) at a 0.2 C rate is close to the AB_5 alloy electrode (298 mAh/g); but the charge voltage of the composite electrode is higher than the AB_5 alloy electrode, and the discharge voltage of the former is lower than the latter. These results indicate that after being compounded with AB_5 alloy, the binding between H_2 molecules (or H atoms) and the graphite surface might be enhanced, thereby leading to a good discharge capacity; but as the electrochemical reduction/oxidation between H_2O and H occurs more difficultly on the surface of graphite than AB_5 alloy, there is higher charge–discharge polarization on the composite electrode. On the other hand, as shown in Fig. 4, during the first 0.2 C charge–discharge cycle, the discharge capacity of

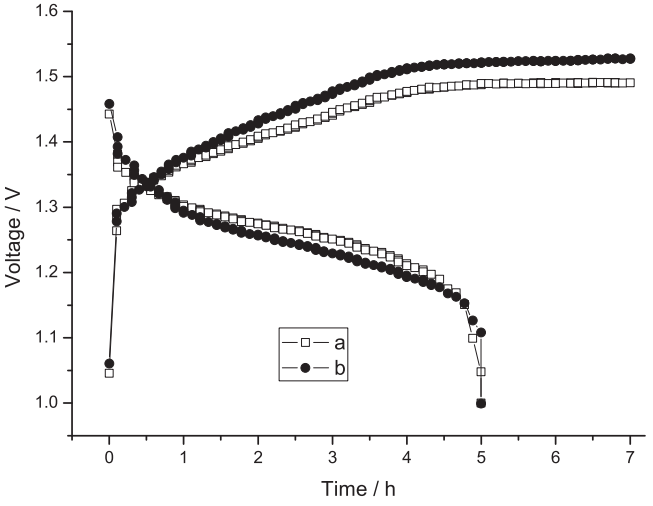

Fig. 3. Typical charge–discharge curves of the simulated batteries at a 0.2 C rate with (a) the AB_5 alloy electrode and (b) the graphite/AB_5 alloy (90 wt%) composite electrode.

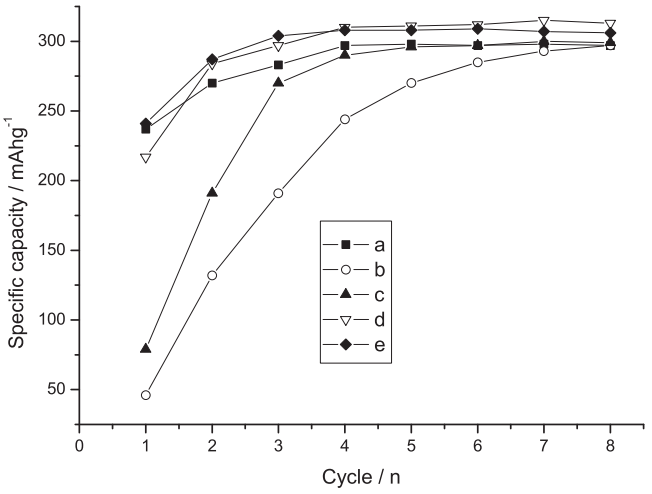

Fig. 4. Discharge capacity of different negative electrodes at a 0.2 C rate (a) the AB_5 alloy electrode and (b–e) the graphite/AB_5 alloy (90 wt%) composite electrodes, where (b) untreated graphite (c) graphite modified with 10 wt% nickel powder (d) graphite modified with 20 wt% nickel powder and (e) graphite modified with 30 wt% nickel powder.

the composite electrode is only 46 mAh/g, and after 7–8 cycles, it reaches the maximum discharge capacity. For the AB_5 alloy electrode, its discharge capacity is 237 mAh/g in the first cycle, and it reaches the maximum discharge capacity only after 3–4 cycles. The difficulty in activation would block the application of the composite electrode in the alkaline secondary batteries.

In order to overcome the difficulty in activation for the graphite/AB_5 alloy composite electrode, graphite was modified by ball milling with different amounts of metal nickel powder. As shown in Fig. 4, the cycles needed for the activation of the composite electrodes decrease with the increase in the addition amount of nickel powder, and when the addition amount is 20 wt%, it is similar to the AB_5 alloy electrode. On the same time, the discharge capacity at a 0.2 C rate of the composite electrode reaches to 315 mAh/g, which is larger than the AB_5 alloy electrode of 298 mAh/g.

Fig. 5 shows the SEM images of the graphite particles before and after being modified with 20 wt% nickel powder. It is clear that metal nickel powder with the size about 1 μm disperses among the plate graphite particles, which could be a good catalyst for the electrochemical reduction/oxidation between H_2O and H. As shown in Fig. 6, after graphite being modified with metal nickel powder, the charge voltage of the simulated batteries declines with the increase in the addition amount of nickel powder, and the discharge voltage ascends simultaneously. This indicates the good catalysis of nickel powder for the electrochemical reduction/oxidation reaction on the surface of graphite. The experimental results show that the appropriate addition amount is 20 wt%. Otherwise, there would be insufficient catalytic sites at lower amounts or excessive non-active material in the electrode at higher amounts.

Different composite electrodes of modified graphite/AB_5 alloy (95 wt%, 90 wt% or 80 wt%) were prepared and their electrochemical properties were tested. As shown in Fig. 7, the composite electrodes with 5 wt% and 10 wt% modified graphite have similar electrochemical properties, but the latter is more economic. The discharge capacity of the composite electrode with 20 wt% modified graphite decreases obviously, which might suggest the insufficient enhancement of the binding between H_2 molecules (or H atoms) and the graphite surface by AB_5 alloy.

Finally, high-power performance of the composite was tested. As shown in Fig. 8, compared to the simulated battery with the AB_5 alloy electrode, the battery with the composite electrode of

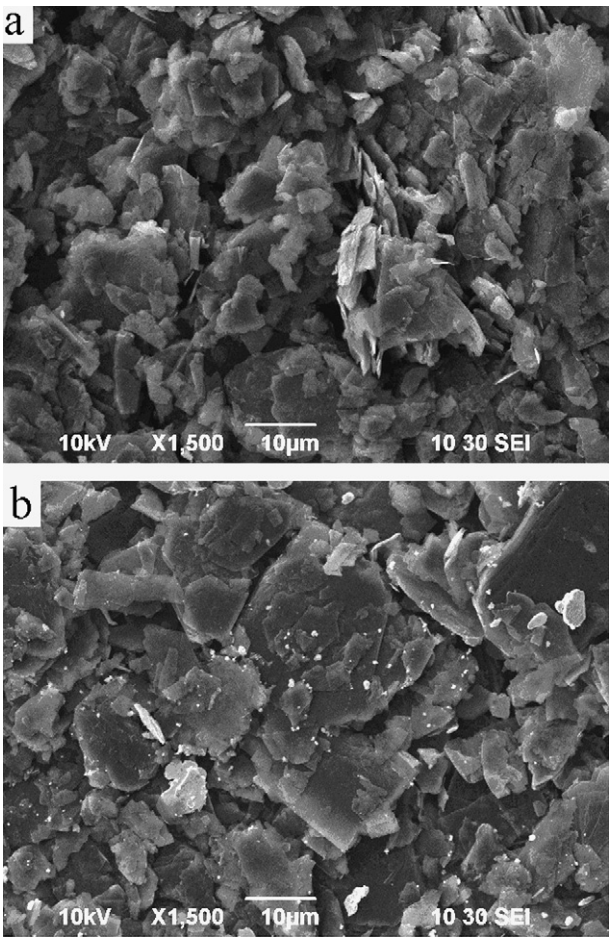

Fig. 5. SEM images of the graphite particles (a) untreated and (b) modified with 20 wt% nickel powder.

modified graphite/AB_5 alloy (90 wt%) has better high-power performance, especially when discharging at a 3 C rate, the discharge capacity of the latter increases 22% and the discharge voltage of the latter obviously exceeds the former.

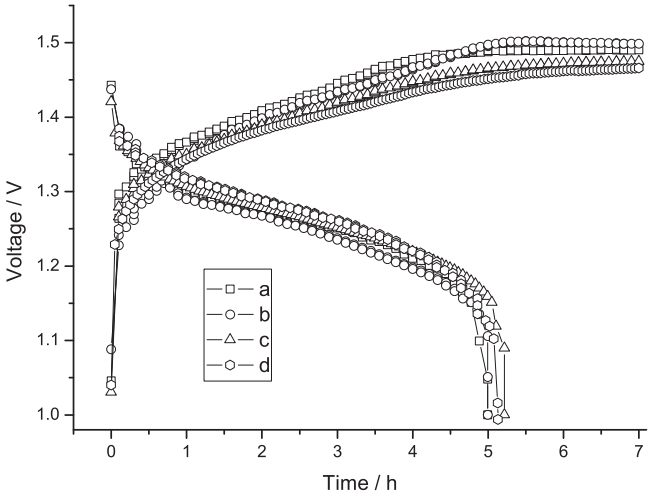

Fig. 6. Typical charge–discharge curves of the simulated batteries at a 0.2 C rate with (a) the AB_5 alloy electrode and (b–d) the graphite/AB_5 alloy (90 wt%) composite electrodes, where (b) graphite modified with 10 wt% nickel powder (c) graphite modified with 20 wt% nickel powder and (d) graphite modified with 30 wt% nickel powder.

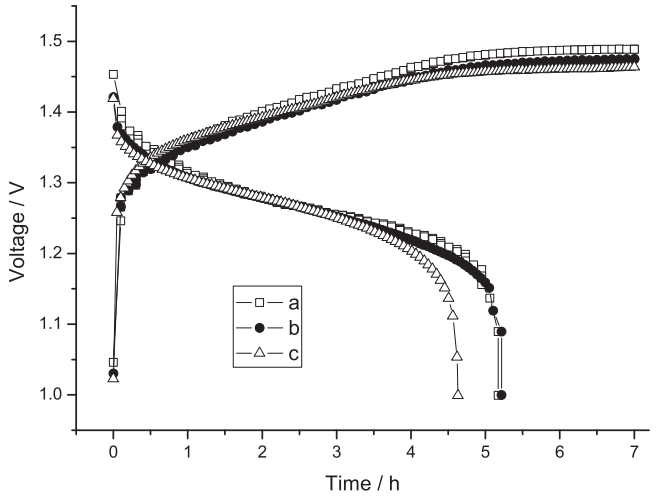

Fig. 7. Typical charge–discharge curves of the simulated batteries at a 0.2 C rate with (a) the graphite/AB_5 alloy (95 wt%) composite electrode, (b) the graphite/AB_5 alloy (90 wt%) composite electrode and (c) the graphite/AB_5 alloy (80 wt%) composite electrode, where graphite is modified with 20 wt% nickel powder.

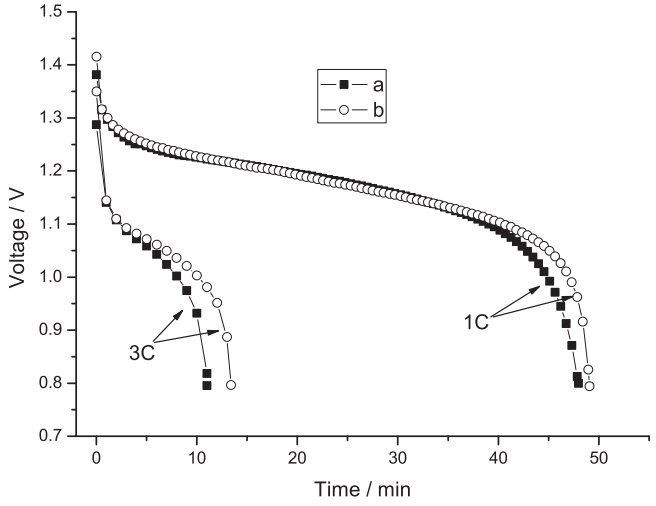

Fig. 8. Typical charge–discharge curves of the simulated batteries at a 1 C or 3 C rate with (a) the AB_5 alloy electrode and (b) the graphite/AB_5 alloy (90 wt%) composite electrode, where graphite is modified with 20 wt% nickel powder.

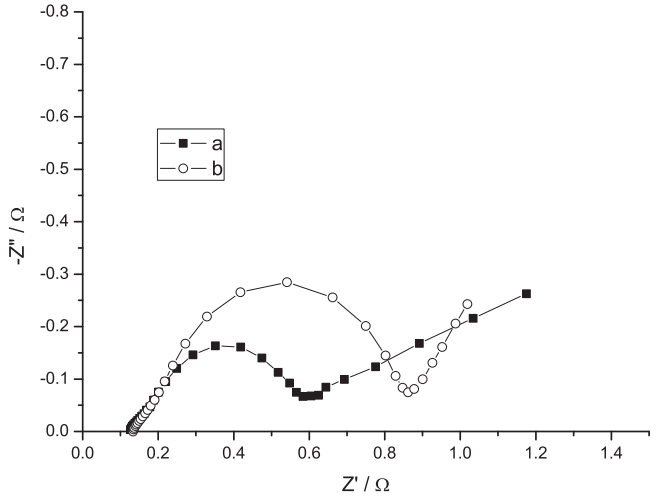

Fig. 9. Impedance plots of the negative electrodes (discharged to 50% depth of discharge) in 7 mol l^{-1} KOH electrolytes at a frequency range from 10^5 to 10^{-2} Hz: (a) the AB_5 alloy electrode and (b) the graphite/AB_5 alloy (90 wt%) composite electrode, where graphite is modified with 20 wt% nickel powder.

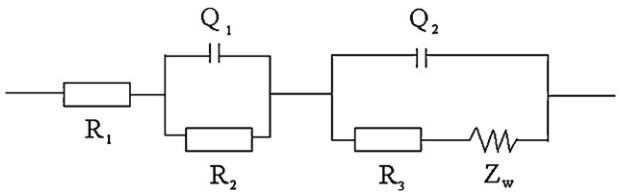

Fig. 10. Proposed equivalent circuit for the MH electrode. R_1: resistance of electrolyte. R_2: contact resistance between alloy particle and current collector. R_3: charge transfer resistance at interface of electrode/electrolyte. Q_i: constant phase element. Z_w: Warburg impendence of hydrogen diffusion.

Fig. 9 shows the impedance plots for the negative electrodes discharged to 50% depth of discharge (DOD) in the 7 mol l^{-1} KOH electrolytes. The plots exhibit three arcs in the whole frequency range. For a MH electrode, the semicircle in high-frequency region is attributed to the contact resistance between the alloy particle and the current collector; the other semicircle in low-frequency region is attributed to a charge transfer process on the electrode surface, and the slope is caused by the diffusion of hydrogen in the alloy [11,12]. A proposed equivalent circuit for the frequency response of the negative electrode is given in Fig. 10. The results of a curve fitting show that the charge transfer resistance R_3 of the composite electrode (0.596 Ω) is larger than the AB_5 alloy electrode (0.424 Ω), which indicates that even after being modified with metal nickel powder, the electrochemical reaction activity on the surface of graphite is lower than AB_5 alloy. But compared with the AB_5 alloy electrode, the Y_w of the composite electrode increases obviously from 17.3S to 29.5S, resulting in an improved hydrogen atom's diffusion ability. As hydrogen diffusion in the bulk of the alloy is a limiting step in the reaction mechanisms of the metal hydride electrode, more rapid diffusion could conduce to better electrochemical properties of the electrode, especially discharge performance at large currents.

The composite electrode of modified graphite/AB_5 alloy (90 wt%) prepared in this paper shows a higher 0.2 C capacity (315 mAh/g) and better high-power performance than the AB_5 alloy electrode. On the other hand, graphite is cheaper than AB_5 alloy and the modification method of ball milling is simple, thus it is suitable for the alkaline secondary batteries.

4. Conclusion

(1) Both the untreated graphite electrode and the metal nickel modified graphite electrode have poor electrochemical hydrogen absorbing performance.
(2) For the untreated graphite/AB_5 alloy (90 wt%) composite electrode, the results of the charge–discharge tests show that its 0.2 C capacity is close to AB_5 alloy electrode (298 mAh/g), but it has higher charge–discharge polarization and difficulty in activation.
(3) With the good catalysis of nickel powder for the electrochemical reduction/oxidation reaction on the surface of graphite, the composite electrode of modified graphite/AB_5 alloy (90 wt%) has a 0.2 C capacity of 315 mAh/g. Compared to the AB_5 alloy electrode, it has lower charge–discharge polarization and its discharge capacity at a 3 C rate increases 22%.
(4) The EIS tests show that hydrogen diffusion in the composite electrode of modified graphite/AB_5 alloy (90 wt%) is more rapid than AB_5 alloy, which benefits its charge–discharge performance.

References

[1] Y. Kojima, Y. Kawai, A. Koiwai, N. Suzuki, T. Haga, T. Hioki, K. Tange, J. Alloy Compd. 421 (2006) 204–208.

[2] P. Hou, S. Xu, Z. Ying, Q. Yang, C. Liu, H. Cheng, Carbon 41 (2003) 2471–2476.
[3] K. Shindoa, T. Kondo, M. Arakawa, Y. Sakurai, J. Alloy Compd. 359 (2003) 267–271.
[4] A.M. Rashidi, A. Nouralishahi, A.A. Khodadadi, Y. Mortazavi, A. Karimi, K. Kashefi, Int. J. Hydrogen Energy 35 (2010) 9489–9495.
[5] C. Carpetis, W. Peschka, Int. J. Hydrogen Energy 5 (1980) 539–554.
[6] W-C. Xu, K. Takahashi, Y. Matsuo, Y. Hattori, M. Kumagai, S. Ishiyama, K. Kanekoc, S. Iijima, Int. J. Hydrogen Energy 32 (2007) 2504–2512.
[7] E. Yoo, L. Gao, T. Komatsu, N. Yagai, K. Arai, T. Yamazaki, K. Matsuishi, T. Matsumoto, J. Nakamura, J. Phys. Chem. B 108 (2004) 18903–18907.
[8] H.-S. Kim, H. Lee, K.-S. Han, J.-H. Kim, M.-S. Song, M.-S. Park, J.-Y. Lee, J.-K. Kang, J. Phys. Chem. B 109 (2005) 8983–8986.
[9] E. Díaz, M. León, S. Ordóñez, Int. J. Hydrogen Energy 35 (2010) 4576–4581.
[10] S-J. Park, S-Y. Lee, Int. J. Hydrogen Energy 35 (2010) 13048–13054.
[11] W. Chen, J. Power Sources 90 (2000) 201–205.
[12] H. Yang, Y. Chen, M. Tao, C. Wu, J. Shao, G. Deng, Electrochim. Acta 55 (2010) 648–655.